JOURNAL OF Materials CHEMISTRY

Nickel complexed within an azamacrocycle as a structure directing agent in the crystallization of the framework metalloaluminophosphates STA-6 and STA-7

Raquel Garcia,[a] Eilidh F. Philp,[a] Alexandra M. Z. Slawin,[a] Paul A. Wright*[a] and Paul A. Cox[b]

[a]*School of Chemistry, University of St. Andrews, The Purdie Building, North Haugh, St. Andrews, Fife, UK KY16 9ST. E-mail: paw2@st-andrews.ac.uk*
[b]*Centre for Molecular Design, University of Portsmouth, King Henry Building, King Henry I Street, Portsmouth, Hants, UK PO1 2DY*

Received 7th December 2000, Accepted 1st March 2001
First published as an Advance Article on the web 29th March 2001

Nickel complexed with the azamacrocycle 1,4,8,11-tetramethyl-1,4,8,11-tetraazacyclotetradecane (tmtact) acts to direct the crystallisation of metalloaluminophosphate (MAPO, M = Mg, Mn, Co, Zn) and silicoaluminophosphate (SAPO) gels to an orthorhombic variant of the STA-6 material (structure code SAS) and to mixtures of this phase with STA-7 (structure code SAV). Compositional analysis, diffuse reflectance UV-visible spectroscopy, magnetic susceptibility and solid state NMR of pure STA-6 samples show that the nickel remains complexed within the macrocycle after crystallisation, adopting square planar geometry. The positive charge on the divalent complex is balanced by the negative charge imparted to the framework by the aliovalent substitution of divalent cations for aluminium or the incorporation of silicon for phosphorus. Crystallographic analysis of a single crystal of the Ni(tmtact)–CoAPO form of STA-7 (*P*4/*n*, $a = 18.684(1)$ Å, $c = 9.408(1)$ Å) is able to locate the complex, disordered about the 4-fold axis, within supercages in the structure. The inorganic framework of the Ni(tmtact)$^{2+}$-templated STA-6 solids remains intact as the organics are removed by calcination, and the STA-6 becomes tetragonal. The paramagnetic Ni^{2+} cations are left within the pore structure. Reduction of the calcined sample in hydrogen at temperatures of 473–523 K gives Ni(I), as shown by ESR spectroscopy, $g = 2.09$.

Introduction

Amine complexes including a range of metals have been shown to direct the crystallisation of aluminophosphate and gallophosphate solids. Complexes of Co(III) with chelates such as diaminoethane[1–3] and diethylenetriamine[4] have been shown to give layered and framework phosphates, some of them chiral. Cobalt(III) and iridium(III) complexes with the secondary amine *trans*-1,2-diaminocyclohexane have been shown[5] to remain intact in syntheses of aluminophosphates, where they form hydrogen-bonded complexes with chains of stoichiometry $[Al_2P_3O_{12}]^{3-}$, and nickel(II) diaminoethane complexes are found to crystallise in the layered aluminophosphate $NiAl_3P_4O_{18}C_4H_{21}N_4$.[6] Cobalt, nickel, copper and gallium complexes of cyclam (1,4,8,11-tetraazacyclotetradecane) give chain and framework phosphates where the metal is bound also to the phosphate oxygens[7–10] and the secondary nitrogens of the complexes form hydrogen bonds with phosphate oxygens of the inorganic network.

In all the cases cited above, removal of the organic ligands results in collapse of the structure. The use of organometallic cobaltocenium ions and their derivatives in the synthesis of aluminosilicates and aluminophosphates, however, gives frameworks that are stable to the removal of organics. Examples include the novel extra-large pore aluminosilicate UTD-1, which is prepared in the presence of decamethylcobaltocenium ions,[11] and $AlPO_4$-16, an aluminophosphate with a cage structure prepared in the presence of cobaltocenium ions.[12] In these cases the complexes act like large inorganic cations, and do not form strong directional bonds with the framework oxygens. As a consequence, fully tetrahedrally-connected frameworks crystallise around them. Removal of the organic part of the complex by heating in oxygen leaves the framework intact and the metal remains within the pore structure. The process is therefore a potentially useful two-step route to catalytic solids normally prepared by synthesis, calcination and cation exchange.

Azamacrocycles with tertiary nitrogens have been found to be effective templates for the synthesis of aluminophosphate-based solids, including VPI-5,[13] MAPO-18,[10] STA-6 and STA-7.[14,15] 1,4,8,11-Tetramethyl-1,4,8,11-tetraazacyclotetradecane (tmtact) is of particular interest, giving rise to either STA-6 or STA-7 depending on the divalent metal cation present in the synthesis gel.[15] In the presence of Mg^{2+}, Mn^{2+} or Fe^{2+}, STA-6 is always the major phase prepared whereas in the presence of Co^{2+} or Zn^{2+}, STA-7 is strongly favoured. In these cases, the metal cation is found ultimately to adopt tetrahedral sites within the framework, although an intermediate stage where the metal is complexed in the amine during crystallisation and thereby controls which phase is formed cannot be ruled out. In a separate experiment the addition of nickel acetate to the gel was found to give a diamagnetic microcrystalline solid of unknown structure. This suggested that the nickel remains complexed within the tmtact in square planar geometry after crystallisation, rather than occupying tetrahedral framework sites.

Rajic *et al.*[16] have shown that the octahedral complex of nickel with tris(2-aminoethyl)amine is included in the channels of $AlPO_4$-5 during crystallisation. In this case the complex does not strongly template the phase that forms, but becomes entrained within the channels upon crystallisation. The same group have also shown[17] that the nickel complex $Ni(en_2(OH)_2)$

can act as a structure directing agent in the formation of AlPO-34 (CHA topology) with a triclinic unit cell distorted away from rhombohedral symmetry due to the presence of the hydroxyl groups which are attached to framework aluminium. In syntheses of nickel aluminophosphates using secondary and tertiary amines as templates,[18–20] the nickel is found to show quite different behaviour, substituting at low levels (2% or less) in the framework to give pale violet solids. ESR and electron spin echo modulation measurements have been taken to suggest[20] that it substitutes for phosphorus. In our work we have studied the synthesis of substituted metallo- and silicoaluminophosphate structures in the presence of tmtact complexed with Ni^{2+} in the gel, and have found that this complex favours the crystallisation of structures with the STA-6 framework over those with the STA-7 structure. We also report here that after crystallisation of either STA-6 or STA-7 in the presence of both nickel and tmtact, nickel is complexed within the macrocycle in square planar geometry rather than substituting in tetrahedral sites within the framework. Calcination of these solids in oxygen gives stable porous frameworks in which the amine has been stripped from the nickel complex.

The reductive behaviour of divalent nickel present as extraframework or framework species within aluminophosphate-based solids has been studied extensively by electron spin resonance.[18,19] These studies have shown that the divalent nickel can be reduced to Ni(I) by suitable reduction treatments, and nickel in this oxidation state within the pores of microporous solids is known to be an active catalyst for such reactions as oligomerisation of ethylene and propylene and cyclotrimerisation of acetylene.[21–23] Here we describe preliminary studies of the reducibility of the nickel that remains after calcination of the solids prepared containing the Ni–tmtact complexes.

Experimental

Sample preparation

Aluminophosphate-based gels with starting compositions given in Tables 1 and 2 were treated hydrothermally. Two series of experiments were performed using tmtact as a template, with and without nickel acetate added to the starting mix. Metalloaluminophosphate (MAPO, M = Mg, Mn, Co, Zn) and silicoaluminophosphate (SAPO) gels were examined. In these cases the molar ratio of macrocycle to nickel was between 3 : 1 and 8 : 1, the excess amine being required to adjust the pH to 7, suitable for the synthesis of framework aluminophosphates. In a typical preparation of Ni-SAPO STA-6, 0.21 g of phosphoric acid (85%, Prolabo) was mixed with 17.56 g of water and 0.26 g of tmtact (Aldrich) was added. To this solution, 0.24 g of aluminium hydroxide hydrate (Aldrich), 0.0765 g of nickel acetate tetrahydrate (Aldrich) and 0.038 g of fumed silica (Sigma) were added and stirred for one hour until homogeneous. The final pH was 7 and the molar ratios in the gel 0.25 NiO : 1 Al_2O_3 : 0.75 P_2O_5 : 0.50 SiO_2 : 0.8 R : 800 H_2O. The gel was loaded in a Teflon-lined stainless steel autoclave and heated for 2 days at 190 °C.

A separate series of experiments was performed where pre-prepared Ni^{2+}-macrocycle complex was added to silicoaluminophosphate gels and the pH adjusted to 7 by addition of tetramethylammonium or tetraethylammonium hydroxides. Control experiments were performed in the absence of nickel. These experiments were performed to determine whether the nickel complex was an effective structure directing agent in the presence of alkylammonium cations commonly used for this purpose. In all cases the reaction products were sonicated and the crystalline fraction separated from amorphous gel in this way was washed with distilled water and dried.

Sample characterisation

All crystalline products were examined by X-ray powder diffraction on a STOE STADIP diffractometer operating on monochromated Cu $K_{\alpha 1}$ radiation. All X-ray powder diffraction data shown in this work were collected in Debye–Scherrer geometry in 0.7 mm silica glass capillaries over 16 hours. Selected area analyses of the products were performed using energy-dispersive analysis of emitted X-rays (EDX) on a JEOL 2010 TEM with a Link analyser. Crystals of nickel-containing Co-STA-7 were of sufficient quality for single crystal analysis.

Samples that were phase pure were examined by TGA and their organic content measured by a Carlo Erba CHN elemental analyser. For selected crystalline products, in order to determine whether the tmtact had been incorporated intact, the inorganic framework was dissolved in 5 M HCl and the liberated amines analysed by NMR spectroscopy according to published procedures. ^{13}C NMR spectra were recorded at 75 MHz on a Bruker AM300 instrument using sodium 3-trimethylsilylpropane sulfonate as the reference. Selected phase pure samples were analysed by ICP-AES following dissolution in aqueous hydrochloric acid and also by solid state NMR. MAS NMR measurements were performed using a Varian 300 MHz spectrometer. ^{13}C CP MAS NMR spectra were obtained under the following conditions: contact time 1 ms, acquisition time 20 ms, recycle delay 1 s, spinning speed 4.1 kHz. ^{31}P and ^{27}Al MAS NMR were performed using a spinning rate of 12 kHz and acquisition times and relaxation delays of 20 ms, 300 s and 5 ms, 0.2 s, respectively. Chemical shifts were referenced to a 85 wt% solution of H_3PO_4 and to $[Al(H_2O)_6]^{3+}$. ^{29}Si MAS NMR was collected using cross polarisation from protons, contact time 3 ms, acquisition time 20 ms, relaxation delay 1 s. TMS was used as the reference for ^{13}C and ^{29}Si chemical shifts.

Magnetic susceptibility measurements were performed on a

Table 1 Gel compositions and crystalline products of hydrothermal syntheses using 1,4,8,11-tetramethyl-1,4,8,11-tetraazacyclotetradecane (tmtact)

Material	Cation ratio in gel	tmtact	H_2O	Unit cell composition	Product	Ref.
MgAlPO	0.2 Mg : 0.8 Al : 1.0 P	0.5	400	$(Mg_{0.2}Al_{0.8}PO_4)_{16}\cdot 1.5R\cdot 2.5H_2O$	STA-6	15
Ni–MgAlPO	0.2 Mg : 0.8 Al : 1.0 P : 0.05 Ni	0.4	400	$(Ni_{0.09}Mg_{0.12}Al_{0.97}PO_4)_{16}$ (by EDX)	STA-6(orth)	This work
ZnAlPO	0.2 Zn : 0.8 Al : 1.0 P	0.5	400	$(Zn_{0.2}Al_{0.8}PO_4)_{24}\cdot 2.6R\cdot 10H_2O$	STA-7	15
Ni–ZnAlPO	0.125 Zn : 0.75 Al : 1.0 P : 0.125 Ni	0.4	400	$(Ni_{0.09}Zn_{0.2}Al_{0.8}PO_4)_{16}\cdot 1.6R\cdot 4H_2O$	STA-6(orth)	This work
MnAlPO	0.2 Mn : 0.8 Al : 1.0 P	0.5	400	—	STA-6	15
Ni–MnAlPO	0.2 Mn : 0.8 Al : 1.0 P : 0.10 Ni	0.4	400	—	STA-6(orth)	This work
CoAlPO	0.2 Co : 0.8 Al : 1.0 P	0.5	400	$(Co_{0.2}Al_{0.8}PO_4)_{24}\cdot 2.3R\cdot 9H_2O$	STA-7	15
Ni–CoAlPO	0.125 Co : 0.75 Al : 1 P : 0.125 Ni	0.4	400	EDX only, see text	STA-6(orth) + STA-7 + impurity	This work
SAPO	1 Al : 0.80 P : 0.20 SiO_2	0.4	400	—	STA-6	This work
Ni–SAPO	1 Al : 0.75 P : 0.25 SiO_2 : 0.125 Ni	0.4	400	$(Ni_{0.11}Si_{0.3}P_{0.7}AlO_4)_{16}\cdot 1.6R\cdot 4H_2O$(ICP&EDX)	STA-6(orth)	This work

All gels were heated at 190 °C for two days, except that with SAPO composition which was heated at 190 °C for seven days. STA-6 samples prepared in the presence of nickel show an orthorhombic distortion (orth). All compositions from a combination of ICP, CHN and TGA analyses, unless stated otherwise.

Table 2 Gel compositions and and crystalline products of hydrothermal synthesis of silicoaluminophosphates using tmtact in the presence of additional bases to control pH to 7–8, and with and without added nickel

Material	Composition	Product	Yield on P (%)	Yield on tmtact (%)
Ni–SAPO[a]	0.125 Ni : 1 Al : 0.75 P : 0.25 SiO_2 : 400 H_2O : 0.4 tmtact	STA-6	63	17
Ni–SAPO[a]	0.125 Ni : 1 Al : 0.75 P : 0.25 SiO_2 : 400 H_2O : 0.125 tmtact : 0.51 TMAOH	STA-6	45	38
Ni–SAPO[a]	0.125 Ni : 1 Al : 0.75 P : 0.25 SiO_2 : 400 H_2O : 0.125 tmtact : 0.53 TEAOH	STA-6/STA7 ~ 50%	18	15
SAPO[b]	1 Al : 0.8 P : 0.20 SiO_2 : 400 H_2O : 0.125 tmtact : 0.5 TMAOH	SAPO-20	—	—
SAPO[b]	1 Al : 0.8 P : 0.20 SiO_2 : 400 H_2O : 0.125 tmtact : 0.5TEAOH	SAPO-39	—	—

[a]2 days at 190 °C. [b]7 days at 190 °C.

Johnson Matthey balance operating according to a modified Gouy method. UV-visible spectrometry was performed in diffuse reflectance mode. ESR spectra were collected on a Bruker EMX 10/12 spectrometer operating at 9.5 GHz with a 100 kHz modulation, with a sweep width of 2000 G, field modulation amplitude 5 G_{pp} and power 10 mW. Samples were in powder form within a 4 mm o.d. quartz tube in the resonant cavity.

Single crystal crystallography and computer simulation

A single dark blue crystal of Ni–CoAPO–STA-7 was selected on the basis of its shape (a block) from a mixture of STA-7 and smaller STA-6 crystals of this composition prepared as described elsewhere in the text. It was examined on a Bruker SMART CCD diffractometer using Mo K_α. Experimental details of the crystallographic analysis are given in Table 3. The framework structure (composition *ca.* $Co_{0.25}Al_{0.75}PO_4$ from EDX measurements) was solved using the SHELXTL[24] package and refined fully anisotropically in *P*4/*n*. Co, Al and P were found to be strictly ordered on alternate tetrahedrally-coordinated sites (average bond lengths: (Co,Al)–O 1.75(2) Å, P–O 1.51(1) Å). The position of the nickel cation was readily determined from the difference Fourier synthesis and refined with full occupancy. The positions of nitrogen were also successfully refined, fully occupying a site with 4-fold multiplicity around the nickel. Additional electron density around the NiN_4 core was refined as carbon atoms of the macrocycle.

CCDC reference number 158125. See http://www.rsc.org/suppdata/jm/b0/b009813m/ for crystallographic files in CIF or other electronic format.

Although microcrystals of Ni–MgAPO–STA-6 of sufficient size for single crystal diffraction were obtained, they were found by single crystal diffraction to have a complex domain structure.

Computer simulation of the location of the Ni(tmtact)$^{2+}$ complex in the cage of STA-7 was performed by a combined Monte Carlo docking and subsequent Simulated Annealing approach. Experimental evidence (crystallography, UV-visible spectroscopy and magnetic measurements) indicates that the nickel possesses square planar coordination with four nitrogens, so the Ni–N_4 core of the complex in the simulations was constrained to have that geometry by the imposition of a harmonic restraint function with a high force constant ($K = 1000$ kcal mol^{-1} Å^{-1}). Calculations were performed using the CVFF Constant Valence Force Field within the program Discover[25] as described previously.[15] Although complexation of Ni^{2+} by tmtact in aqueous solution gives exclusively the *trans*-I (*R*,*S*,*R*,*S*) conformation (all four methyl groups on the same side of the complex), it can equilibrate under suitable conditions with the *trans*-III (*R*,*S*,*S*,*R*) configuration (two methyl groups on each side of the ring). In these solution studies the nickel is also coordinated by additional ligands from the solution.[26] Energy minimisation studies[27] have suggested that the more favourable geometry when the nickel is only four-fold coordinated is the *trans*-I configuration. The lowest energy positions of the *trans*-I and *trans*-III configurations within the STA-7 cage were therefore modelled and compared with the results of crystallographic analysis.

Table 3 Experimental crystallographic details for Ni–CoAPO–STA-7

Crystal system	Tetragonal
Space group	*P*4/*n*
Composition	$Ni_{0.1}Co_{0.2}Al_{0.8}PO_4 \cdot xR \cdot yH_2O$
Crystal dimensions/μm	30 × 30 × 100
T/K	293
μ/mm^{-1}	1.32
λ/Å	0.71073
a/Å	18.684(1)
c/Å	9.408(1)
V/Å^3	3284.3(4)
Z	8
R(int)	0.16
Unique reflections	2355
Observed reflections ($>2\sigma$)	1316
R_1	0.078
$wR_2(F^2)$	0.192

Removal of organics by calcination

Selected samples were calcined in flowing dry oxygen at 550 °C for 10 hours. Upon cooling to 160 °C the oxygen gas flow was switched to nitrogen saturated with n-hexane vapour to stabilise the samples against subsequent exposure to atmospheric moisture. These samples were then loaded into capillaries and degassed under a vacuum to remove adsorbed hexane. The capillaries were sealed and X-ray powder diffraction performed in Debye–Scherrer geometry.

In addition, selected nickel-containing samples were calcined in oxygen to remove the template and then reduced in 100 Torr of hydrogen for 1 hour at temperatures between 373 and 520 K and the samples analysed by ESR.

Results and discussion

Synthesis and general characterisation of products

Table 1 details the phases produced by hydrothermal crystallisation of aluminophosphate-based gels with a range of compositions, as determined by X-ray powder diffraction. As seen previously, aluminophosphate gels crystallised in the presence of tmtact to give STA-6 when magnesium or manganese was added and STA-7 when cobalt or zinc was added. Adding silica to the preparations gave the silicoaluminophosphate form of STA-6, reported here for the first time. The SAPO preparations were found to contain SAPO-43 as an impurity phase. Since Si^{4+} does not complex with the tmtact under these conditions, this indicates that a cation–tmtact complex is not essential for the synthesis of the STA-6 structure and that the diprotonated form of tmtact present at these pH's can act as a structure directing agent by itself.

Adding nickel to these preparations gave marked effects in each case. Crystalline products from the Ni–MgAPO, Ni–ZnAPO and Ni–SAPO preparations were orange solids, whereas the Ni–CoAPO solid was dark blue. The presence of nickel in all the samples was confirmed by EDX analysis. Diffuse reflectance UV-visible spectroscopy of the orange

solids reveal absorption maxima at 243 nm and 485 nm, the latter being characteristic of nickel in square planar geometry.[28] No evidence of absorption at a longer wavelength was observed, indicating none of the nickel is in octahedral configuration. Furthermore, magnetic susceptibility measurements of the Ni–MgAPO, Ni–SAPO and Ni–ZnAPO solids showed them to be diamagnetic, which results from the nickel d^8 electronic configuration in square planar geometry. For example, the magnetic susceptibilities of as-prepared Ni–SAPO–STA-6 and Ni–MgAPO–STA-6 are -3×10^{-7} and -1×10^{-7} cgs, respectively. Products of crystallisation of Ni–ZnAPO gels in the presence of typical amine templates such as tripropylamine give light green solids—mixtures of colourless aluminophosphates and poorly crystallised nickel phosphate—which are strongly paramagnetic, as expected for samples containing octahedral nickel.

^{13}C NMR of the organic compounds liberated by dissolution of the aluminophosphate frameworks of nickel-containing aluminophosphates MgAPO–STA-6 and ZnAPO–STA-6 in hydrochloric acid showed (δ 19.5, 45.3, 47.0, 51.9) that the macrocycles are included intact within the framework solids upon crystallisation, as they are for MgAPO–STA-6, ZnAPO–STA-7 and CoAPO–STA-7 prepared without nickel.[15]

Nickel-containing STA-6 samples

Analysis of X-ray diffraction patterns from the Ni–MgAPO, Ni–MnAPO, Ni–ZnAPO and Ni–SAPO preparations suggested that a crystallographic variant of tetragonal STA-6 is prepared in these cases. The new solids can be indexed as orthorhombic and the pattern fitted using the Le Bail routine within the GSAS suite of programs.[29,30] It has not so far been possible to solve the detailed structure of these solids from the X-ray powder data, but systematic absences are consistent with the space group *Pnnm*, which is that expected by loss of the fourfold axis from *P4/mnc*, the space group of STA-6 prepared without nickel. For the Ni–SAPO–STA-6 sample, unit cell values of $a=13.9668(4)$, $b=14.6472(4)$, $c=10.4118(3)$ Å are obtained.

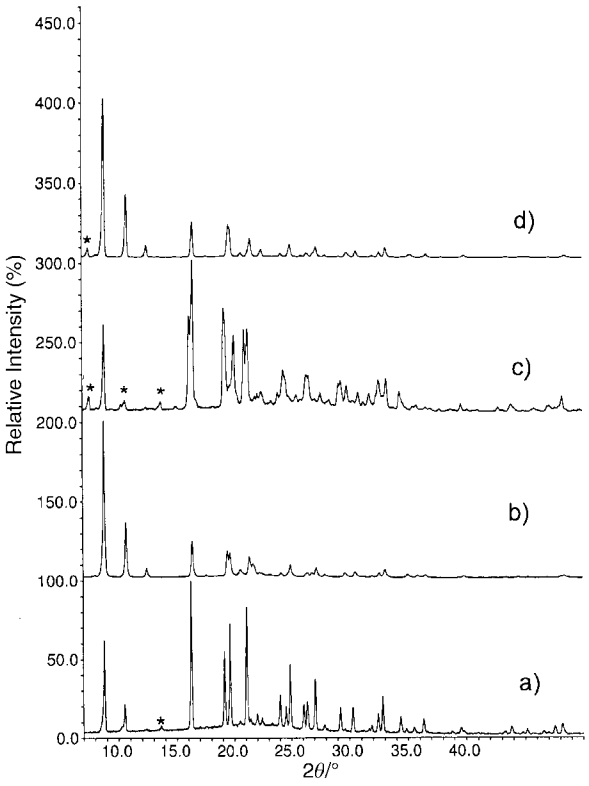

Fig. 1 X-Ray powder diffraction patterns (Cu $K_{\alpha1}$ $\lambda=1.54056$ Å) of (a) as-prepared MgAPO–STA-6, (b) calcined MgAPO–STA-6 (560 °C, 10 h, O_2), (c) as-prepared Ni-MgAPO–STA-6 (showing orthorhombic distortion) and (d) calcined Ni–MgAPO–STA-6. ASterisks indicate peaks from unidentified impurities. The samples were prepared in the presence of tmtact as structure directing agent.

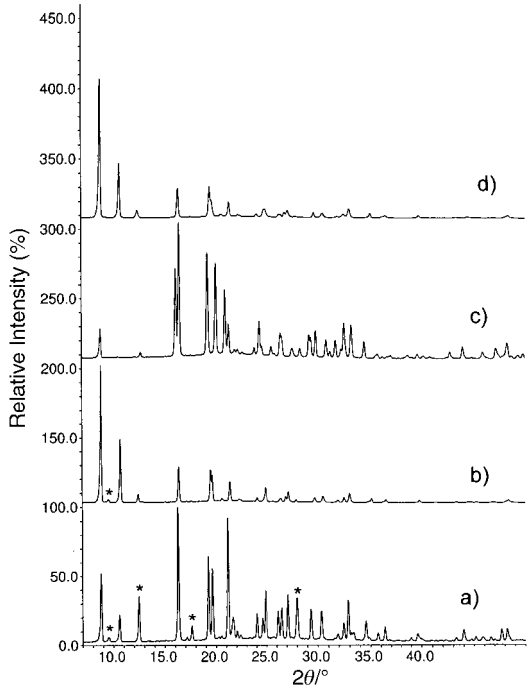

Fig. 2 X-Ray powder diffraction patterns of (a) as-prepared SAPO–STA-6 (SAPO-43 impurity reflections asterisked), (b) calcined SAPO–STA-6, (c) as-prepared Ni–SAPO–STA-6 (orthorhombic) and (d) calcined Ni–SAPO–STA-6.

Diffraction patterns for as-prepared and calcined samples of MgAPO and SAPO solids prepared with and without nickel are shown in Fig. 1 and 2. Calcination of the Ni–MgAPO and Ni–SAPO phases gives solids with diffraction patterns identical to those of calcined samples prepared in the absence of nickel, suggesting that the structures of the as-prepared samples have a similar framework topology to STA-6 prepared without nickel. The nickel complex is responsible for the framework distortion.

Addition of nickel to the SAPO preparation was therefore found to give distorted STA-6. MAS NMR of a phase pure sample of the Ni–SAPO–STA-6 sample gives good quality carbon, phosphorus, silicon and aluminium spectra (Fig. 3a–d) without pronounced sidebands, indicating that the nickel is indeed diamagnetic. The ^{29}Si MAS NMR of this sample (δ −92.7) indicates that all the silicon is surrounded by 4 (–O–Al) linkages in the structure, and therefore substitutes directly for phosphorus in the framework. ^{27}Al MAS NMR indicates that the aluminium occupies mainly tetrahedral but also some octahedral sites (δ 5.7, 30.7), and ^{31}P MAS NMR reveals that all the phosphorus (δ −30.2) is tetrahedrally-coordinated through oxygens to aluminium. In addition the ^{13}C MAS NMR indicates that the macrocycle is incorporated intact, although the chemical shift values (δ 23.3, 45.5, 47.5, 62.6) are different to those observed in MgAPO–STA-6 without nickel (δ 21.0, 43.5, 54.5, 62.8).

For the ZnAPO gels, adding nickel results mainly in the synthesis of small, orange crystals of a crystallographically-distorted variant of the STA-6 structure, although a few larger crystals of STA-7 (tetragonal blocks rather than the elongated tetragonal prisms typical of STA-6) may be observed under the optical microscope. This is in direct contrast to the preparation in the absence of nickel, where ZnAPO–STA-7 is the predominant phase (Fig. 4). This indicates the strongly structure-directing influence of the complex.

The inorganic and organic contents of phase pure Ni–

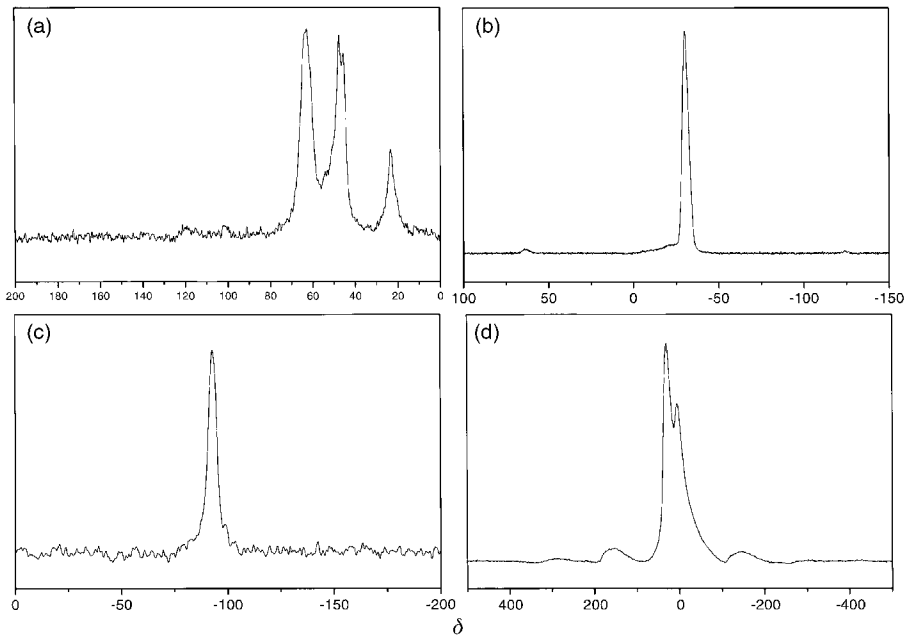

Fig. 3 NMR spectra of Ni–SAPO–STA-b. (a) ^{13}C, (b) ^{31}P, (c) ^{29}Si (CP from ^{1}H) and (d) ^{27}Al.

ZnAPO–STA-6 and Ni–SAPO–STA-6 were measured by ICP-AES and carbon, hydrogen and nitrogen analysis, and TGA was used to determine their water content. The value for silicon in the SAPO was taken from EDX measurements, since not all the silicon was dissolved by HCl solutions used in the ICP analysis. EDX results on Ni, Al and P are within 15% of the values obtained by ICP-AES. EDX analysis was also performed on Ni–MgAPO–STA-6 (Table 1) and on the Ni–CoAlPO–STA-6/7 mixture. In the latter case, all crystals examined contained nickel and cobalt, with Ni/Co ratios of *ca.* 0.6 and Co/P ratios of *ca.* 0.11.

The compositional results show nickel contents far higher than those achieved when nickel substitutes in the framework, and indicate that the divalent charge on the nickel complex balances the negative charge on the framework.

Ni–CoAPO preparations

Adding nickel to a CoAPO gel results in a mixture of dark blue STA-6 and STA-7 crystals, and area selective analysis by EDX in the electron microscope indicates that cobalt and nickel are present in all crystals in similar amounts. The dominance of STA-6 crystals in this mixture contrasts with the synthesis without nickel, where STA-7 is prepared phase pure, and confirms that the presence of the nickel–tmtact complex favours the formation of the orthorhombic STA-6 structure. Whereas single crystal analysis is not possible for the STA-6 crystals, Ni–CoAPO–STA-7 occurs as tetragonal crystals of sufficient size and quality for single crystal structure analysis.

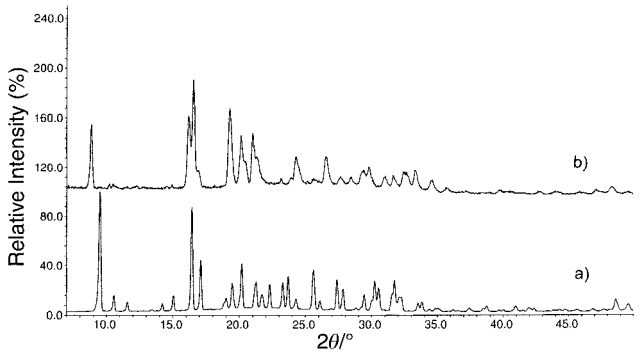

Fig. 4 X-Ray diffraction patterns of (a) as-prepared ZnAPO–STA-7, (b) as-prepared Ni–ZnAPO–STA-6 (orthorhombic). Both samples were prepared in the presence of tmtact.

Single crystal analysis was performed on a tetragonal prism of Ni–CoAPO–STA-7 (See Crystallography section). The structure solution unambiguously locates the cobaltoaluminophosphate framework and the position of the nickel and the surrounding four nitrogen atoms of the macrocycle but the difference in symmetry between the framework (four-fold) and the macrocycle (maximum two-fold) results in static disorder. Consequently, fractionally occupied positions for methyl group carbons are located above and below the ring and the positions of methylene carbons from $-(CH_2)_2-$ and $-(CH_2)_3-$ chains in the ring are superimposed. The Ni–N distances observed for this structure are 1.98(1) Å, typical for nickel complexes of this kind. Fig. 5a and b show the location of the NiN_4 core of the $Ni(tmtact)^{2+}$ complex within the supercage of STA-7 and a configuration of the macrocycle that can be interpolated incorporated most, but not all, of the carbon atoms located in the diffraction experiment.

The positional disorder of the macrocycle complex in the STA-7 supercage renders ambiguous the crystallographic determination of its geometry. The Ni is found to have square planar coordination to nitrogens, and the Ni–N bond lengths (1.98(1) Å), diamagnetism and electronic spectra are consistent with the nickel being four-fold coordinated. We have modelled the cage of STA-7 as described in the experimental section and the favoured geometries of *trans*-I and *trans*-III configurations are given in Fig. 6a and b. They cannot be distinguished on the basis of comparison of the positions of their Ni–N_4 core with that determined experimentally. The location of observed positions of methyl group carbons above and below the ring supports the disordered presence of the *trans*-III isomer but it is possible that the experimental structure contains macrocyclic complexes in both configurations.

Structure direction by the $Ni(tmtact)^{2+}$ complex

The $Ni(tmtact)^{2+}$ complex is shown to have a structure directing influence towards STA-6 in an orthorhombically distorted form. In order to determine whether this influence is greater than that exerted by quaternary ammonium cations, mixtures of $Ni(tmtact)^{2+}$ and TMAOH or TEAOH were added to silicoaluminophosphate gels and heated hydrother-

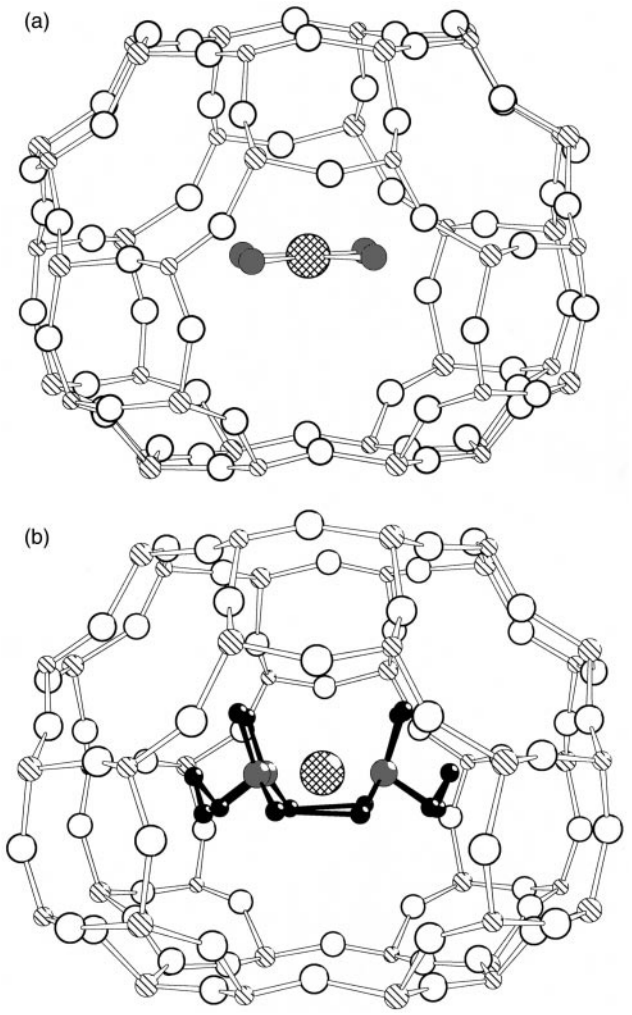

Fig. 5 (a) The position of the NiN_4 core of the $Ni(tmtact)^{2+}$ complex in the STA-7 cage, determined from single crystal diffraction. (b) One possible interpretation of the observed peaks of electron density located around the NiN_4 core of the $Ni(tmtact)^{2+}$ complex. In this case not all the observed electron density peaks refined as carbon atoms have been included in the suggested configuration, which has *trans*-I geometry. The complex may also be present in the *trans*-III configuration. Legend: large double hatched spheres, nickel; grey, nitrogen; black, carbon; small single hatched, phosphorus; medium single hatched, aluminium; large open spheres, oxygen.

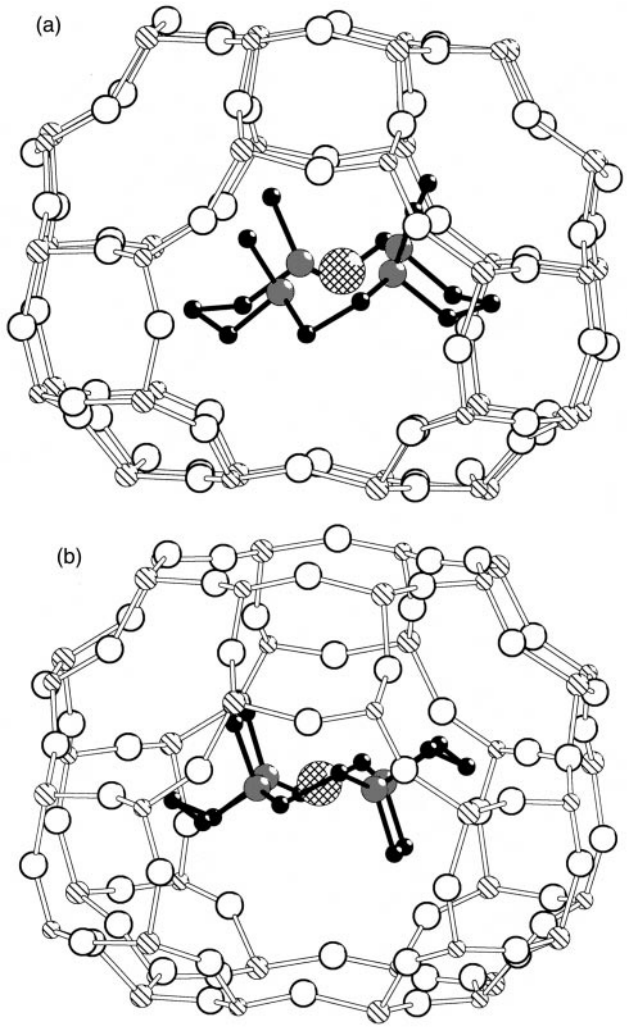

Fig. 6 Energy minimised locations of (a) the *trans*-I and (b) the *trans*-III configurations of the $Ni(tmtact)^{2+}$ complexes within the supercages of STA-7. Legend as for Fig. 5.

mally (Table 2). In each case the only crystalline phases to form were STA-6 or a mixture of STA-6 and STA-7. Repeating the synthesis without the addition of nickel gave SAPO-39 when the added base was TEAOH and SAPO-20 when TMAOH was used. This shows that the complex is a more efficient structure directing agent not only than TMAOH and TEAOH but also than the uncomplexed macrocycle. Furthermore, this permits the synthesis of STA-6 with more efficient use of the tmtact macrocycle (38% *cf.* 17%, Table 2).

The powder diffraction patterns of calcined Ni–MgAPO and Ni–SAPO samples indicate that the framework remains intact upon removal of the organic molecules. In all cases the patterns are similar to those of calcined samples of MgAPO and SAPO samples prepared without nickel. The samples become paramagnetic upon calcination. The magnetic susceptibility of NiSAPO–STA-6, for example, when calcined, is 28×10^{-7} cgs. This confirms that the nickel is no longer square planar, which is expected as the complex is destroyed. It has not been possible to locate unambiguously the location of nickel cations from analysis of the diffraction data. ESR of calcined samples gives no signal, as expected from Ni^{2+}. A strong resonance and some weaker signals are observed as the samples are heated in 100 Torr H_2 at temperatures of 473 K and above. Fig. 7 shows the ESR spectrum collected at 150 K after reduction at 520 K. The main signal, $g = 2.09$, may be attributed to Ni(I) species, according to the work of Kevan.[18,19] This suggests that the Ni(II) species that remain after calcination are accessible to H_2 molecules. Continued heating in hydrogen at 573 K results in the reduction of nickel to nickel metal.

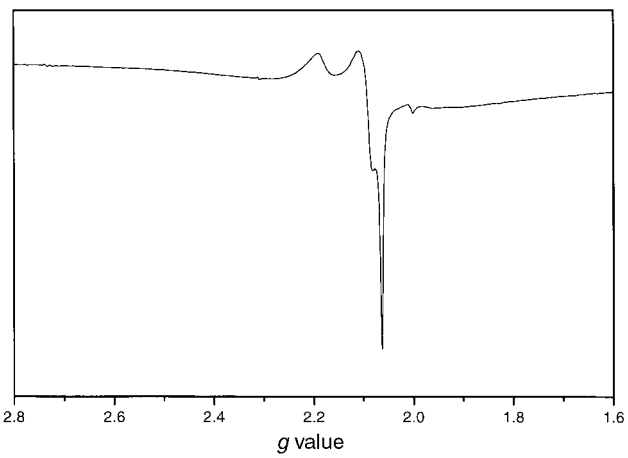

Fig. 7 ESR of Ni–MgAPO–STA-6, calcined, then reduced under hydrogen at 520 K for 1 hour. The ESR was run in hydrogen at 150 K.

Further work is in progress to determine the geometry of the Ni(tmtact)$^{2+}$ complex in the distorted STA-6 structure and the location of nickel in the calcined materials. Studies are also in progress to assess the general potential of this route to the introduction of transition metal cations into extra-framework positions. For aluminophosphate-based solids, this is a more promising route to the inclusion of cations than ion-exchange *via* aqueous solution, because the structures of calcined aluminophosphates are readily hydrolysed. It is also possible to prepare microporous solids with redox active metal cations in both framework and extra-framework sites in this way.

Conclusions

(1) This work demonstrates that nickel is complexed in square planar geometry within the azamacrocycle tmtact during crystallisation of metalloaluminophosphates and silicoaluminophosphates with the STA-6 and STA-7 framework structures. The divalent charge on the complex is balanced by the incorporation of aliovalent cations into the framework that impart to it a negative charge. The solids containing the complex (and no other coloured cations) are orange/salmon pink in colour, absorb at 243 nm and 485 nm in the UV-visible region, and are diamagnetic.

(2) The presence of nickel in the tmtact-templated syntheses of these solids gives a strong preference for the formation of the STA-6 framework structure over the STA-7 structure, and acts as a structure-directing agent. The use of nickel–tmtact complexes therefore permits for the first time the synthesis of pure phases with the STA-6 structure that have the ZnAPO and CoAPO framework compositions. The structures are prepared as orthorhombic variants of the STA-6 structure. This behaviour is similar to that observed in the synthesis of triclinically-distorted AlPO-34 in the presence of diaminoethane complexes of nickel.

(3) The complex of Ni(II) with tmtact is able to introduce nickel into the pore space of metalloaluminophosphates, whereas other divalent metal cations such as Mn, Fe, Co and Zn become incorporated within the tetrahedral cation sites in the framework using the same templates. It is likely that there is competition between the macrocycle and the framework during crystallisation, and that the reluctance of the nickel to adopt a tetrahedral configuration favours its final position in the complex rather than in the inorganic framework.

(4) Calcination of solids with the MgAPO and SAPO framework composition prepared in the presence of the Ni(tmtact)$^{2+}$ complex removes the organic, leaving Ni^{2+} cations within the resultant metalloaluminophosphate pore structures. The nickel no longer possesses square planar geometry, and is therefore paramagnetic, as shown by magnetic susceptibility measurements. Reduction of the nickel in hydrogen at 200 °C and above results in the formation of Ni(I) as seen from ESR, and ultimately metallic nickel at 300 °C. The divalent nickel that is introduced into the pores is therefore accessible to hydrogen.

Acknowledgements

We gratefully acknowledge the University of St. Andrews and EPSRC for supporting this work and thank Dr. David Apperley and the Durham EPSRC solid state NMR facility for performing the MAS NMR spectroscopy. We thank Professor John Walton (St. Andrews) for performing the ESR measurements.

References

1 K. Morgan, G. Gainsford and N. Milestone, *J. Chem. Soc., Chem. Commun.*, 1995, 425.
2 M. J. Gray, J. Jasper, A. P. Wilkinson and J. C. Hanson, *Chem. Mater.*, 1997, **9**, 976.
3 S. M. Stalder and A. P. Wilkinson, *Chem. Mater.*, 1997, **9**, 2168.
4 D. A. Bruce, A. P. Wilkinson, M. G. White and J. A. Bertrand, *J. Solid State Chem.*, 1996, **125**, 228.
5 D. J Williams, J. S. Kruger, A. F. McLeroy, A. P. Wilkinson and J. C. Hanson, *Chem. Mater.*, 1999, **11**, 2241.
6 M. Helliwell, B. Gallois, B. M. Kariuki, V. Kaucic and J. R. Helliwell, *Acta Crystallogr., Sect. B*, 1993, **49**, 420.
7 T. Wessels, L. B. McCusker, Ch. Baerlocher, P. Reinert and J. Patarin, *Microporous Mesoporous Mater.*, 1998, **23**, 67.
8 T. Chatelain, J. Patarin, E. Brendle, F. Dougnier, J. L. Guth and P. Schulz, *Stud. Surf. Sci. Catal.*, 1997, **105**, 173.
9 D. S. Wragg, G. B. Hix and R. E. Morris, *J. Am. Chem. Soc.*, 1998, **120**, 6822.
10 M. J. Maple, E. F Philp, A. M. Z. Slawin, P. Lightfoot, P. A. Cox and P. A. Wright, *J. Mater. Chem.*, 2001, **11**, 98.
11 C. C. Freyhardt, M. Tsapatsis, R. F. Lobo, K. J. Balkus and M. E. Davis, *Nature*, 1996, **381**, 295.
12 K. J. Balkus, A. G. Gabrielov and S. Shepelov, *Microporous Mater.*, 1995, **3**, 489.
13 J. A. Hriljac and T. A. Khan, *Inorg. Chim. Acta*, 1999, **294**, 179.
14 V. Patinec, P. A. Wright, P. Lightfoot, R. A. Aitken and P. A. Cox, *J. Chem. Soc., Dalton Trans.*, 1999, 3909.
15 P. A. Wright, M. J. Maple, A. M. Z. Slawin, V. Patinec, R. A. Aitken, S. Welsh and P. A. Cox, *J. Chem. Soc., Dalton Trans.*, 2000, 1243.
16 N. Rajic, D. Stojakovic, A. Meden and V. Kaucic, *Proc. 12th Int. Zeolite Conf.*, eds. M. M. J. Treacy, B. K. Marcus, M. E. Bisher and J. B. Higgins, MRS, Warrendale, Pennsylvania, 1999, p. 1765.
17 N. Rajic, A. Meden, P. Sarv and V. Kaucic, *Microporous Mater.*, 1998, **24**, 83.
18 N. Azuma, M. Hartmann and L. Kevan, *J. Phys. Chem.*, 1994, **98**, 1221.
19 M. Hartmann, N. Azuma and L. Kevan, *J. Phys. Chem.*, 1995, **99**, 10988.
20 M. Hartmann and L. Kevan, *Chem. Rev.*, 1999, **99**(3), 635.
21 P. Pichat, J. C. Vedrine, P. Gallezot and B. Imelik, *J. Catal.*, 1974, **32**, 190.
22 V. B. Kazansky, I. V. Elev and B. N. Shelimov, *J. Mol. Catal.*, 1983, **21**, 265.
23 L. Bonneviot, D. Olivier and M. Che, *J. Mol. Catal.*, 1983, **21**, 415.
24 G. M. Sheldrick, SHELXTL, version 5.3, Program for the solution of crystal structures, University of Göttingen, 1993.
25 Discover 3.1 program, MSI, San Diego, USA, 1993.
26 P. Moore, J. Sachinidis and G. R. Willy, *J. Chem. Soc., Chem. Commun.*, 1983, 522.
27 T. W. Hambley, *J. Chem. Soc., Dalton Trans.*, 1986, 565.
28 A. B. P. Lever, *Inorganic electronic spectroscopy*, *Studies in Physical and Theoretical Chemistry*, Elsevier, 1984.
29 A. Le Bail, *J. Solid State Chem.*, 1989, **83**, 267.
30 A. C. Larson and R. B. von Dreele, Generalized Crystal Structure Analysis System, Los Alamos Laboratory, USA, 1998.